Analyst

Accepted Manuscript

This article can be cited before page numbers have been issued, to do this please use: W. Na, T. Hu and X. Su, *Analyst*, 2016, DOI: 10.1039/C6AN01087C.

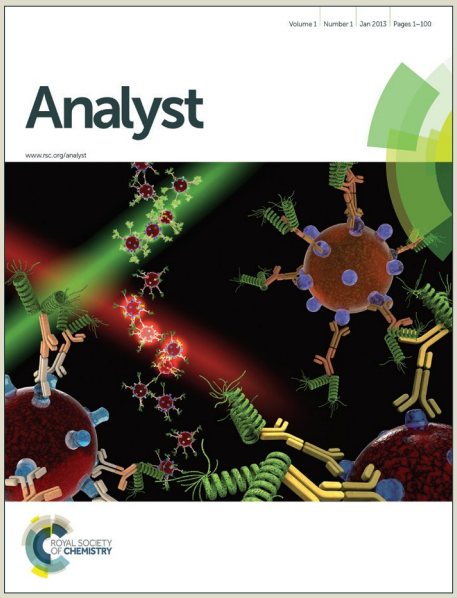

ROYAL SOCIETY OF CHEMISTRY

www.rsc.org/analyst

View Article Online
DOI: 10.1039/C6AN01087C

Sensitive detection of acid phosphatase based on graphene quantum dots nanoassembly

Weidan Na, Tianyu Hu, Xingguang Su *

Department of Analytical Chemistry, College of Chemistry, Jilin University, Changchun, 130012, China

*Corresponding author, Tel.: +86-431-85168352, E-mail address: suxg@jlu.edu.cn

View Article Online
DOI: 10.1039/C6AN01087C

ABSTRACT

In this paper, we reported a convenient label-free fluorescence biosensor for the detection of acid phosphatase based on the aggregation-caused quenching of graphene quantum dots (GQDs). The fluorescence of GQDs could be quenched by poly-(dimethyl diallyl ammonium chloride) (PDDA), the high efficiency of the quenching was caused by the non-covalent binding of positively charged PDDA to the negatively charged GQDs through electrostatic interactions, aggregating to form a GQDs/PDDA complex. And then the addition of sodium hexametaphosphate $(NaPO_3)_6$ could effectively turn on the quenched fluorescence due to the stronger electrostatic interactions between positively charged PDDA and negatively charged $(NaPO_3)_6$. The introduction of acid phosphatase (ACP) would lead to the break down of $(NaPO_3)_6$ into small fragments and disassemble the complex of PDDA/$(NaPO_3)_6$. As a result, the recovered fluorescence could be quenched again by the addition of ACP. Quantitative evaluation of ACP activity in a broad range from 30 nU mL^{-1} to 420 nU mL^{-1} with a detection limit of 12 nU mL^{-1} can be achieved in this way, which endowed the assay with sufficiently high sensitivity for practical detection of ACP in human serum.

Key words: Graphene quantum dots, Aggregation-caused quenching, Acid phosphatase, Florescence detection

View Article Online
DOI: 10.1039/C6AN01087C

Introduction

Acid phosphatase (ACP), a ubiquitous digestive enzyme, has a broad specificity for catalyzing the hydrolysis of phosphate esters under acidic environment.[1] Although the concentration of ACP are found to be normally low in mammalian cells, it is involved in many important physiological processes. It is found that, in the human body, an abnormally elevated level of ACP is closely related to many diseases like prostate cancer, Gaucher disease, and disorders related to kidneys, veins, and bones.[2-3]As a result, ACP is always considered as an important serum marker for related disease and a useful prognostic indicator. Due to its biological and clinical importance, the precise concentration measurement of ACP in blood has been regarded as an essential factor in the pathologic diagnosis of these relative diseases.

To date, a few common methods for ACP assay have been reported, including spectrophotometry,[4] fluorimetry,[5] immunoassay [6] and electrochemical methods.[7] Although these methods offer reasonable sensitivity. However they are usually time-consuming, laborious, and need the separation of be-surveyed substance. Furthermore, some ACP assays need alkaline pH condition, which could be disrupted by alkaline phosphatase. Fluorescent methods for ACP assay will offer new alternatives since they are rapid, continuous, and in real time. In the past few years, fluorescence analysis for some small molecules has shown several unique advantages such as high sensitivity, high selectivity, and easy to operate. Liu et al reported a novel strategy for ACP detection based on the fluorescence of $CuInS_2$ QDs was quenched by sodium hexametaphosphate and restored by ACP who could hydrolyze the sodium hexametaphosphate into small fragments.[8] Xu et al used Squaraine (SQ) dyes whose fluorescence wavelength in the red to NIR region for the determination of ACP and its inhibitor. This design was based on the assembly of probe SQ with

View Article Online
DOI: 10.1039/C6AN01087C

the substrate $(NaPO_3)_6$, which utilizes the aggregation-caused quenching (ACQ) and enzymolysis to trigger the optical response.[9] Yan et al designed a sensitive fluorescent sensing platform for phenol and ACP activity detection based on 3-aminobenzeneboronic acid functionalized $CuInS_2$ QDs.[10] All these methods obtained satisfactory results since the unique optical performance from the semiconductor quantum dots or organic dyes.

GQDs are usually considered as a class of zero-dimensional nanomaterials, which exhibits unique optical properties due to the quantum confinement and edge effects. GQDs have ignited tremendous research interest for their superiority in photostability, excitation-dependent emission tunability, flexibility in surface functionalization, remarkably low cytotoxicity, good cell membrane permeability and excellent biocompatibility.[11-12] GQDs are considered to be competitive alternatives to organic dyes and heavy metal based quantum dots. Up to now, GQDs have been applied in many fields such as sensing, bio-imaging, photovoltaic devices and catalysis.

In this work, we have developed a fast, facile and top-down approach to synthesize orange emission GQDs. The obtained GQDs could be used to fabricate a novel sensing system for the detection of ACP (Scheme 1). Firstly, we utilized a cationic polyelectrolyte PDDA to quench the fluorescence of GQDs via electrostatic interactions to form GQDs/PDDA aggregates. $(NaPO_3)_6$, with six negative charges in the six-membered ring, behaves as a building block to cause the aggregation of positively charged PDDA through intermolecular electrostatic interaction, leading to the disaggregation of GQDs/PDDA complex and the fluorescence recovery of GQDs solution. Then, ACP was added to the detection system, which would hydrolyze $(NaPO_3)_6$ into the phosphate segment. As a result. PDDA would be released from $(NaPO_3)_6$/PDDA complex and the fluorescence of GQDs would be quenched again. Thus, a facile and label-free ACP fluorescent

View Article Online
DOI: 10.1039/C6AN01087C

detection system has been established. It could be used for ACP detection under weak acidic conditions.

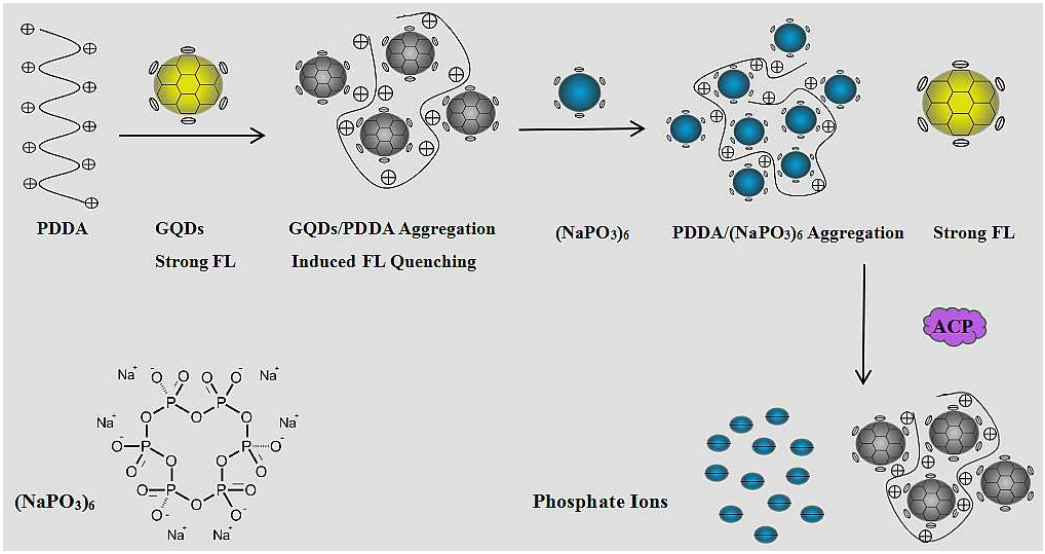

Scheme 1 The presentation of the mechanism for the detection of ACP based on the aggregation of GQDs.

Experimental section

Materials

All reagents were of at least analytical grade. The water used in all experiments had a resistivity higher than 18 MΩ cm^{-1}. Graphite powder (100 mesh), H_2SO_4 (98%), H_2O_2 (30%) and $KMnO_4$ were purchased from HuaCheng Biological Co., Ltd (ChangChun). $(NaPO_3)_6$, ACP and PDDA were purchased from Beijing Dingguo Biotechnology Company. Sodium dehydrogenized phosphate (NaH_2PO_4) and disodium hydrogen phosphate (Na_2HPO_4) were purchased from Beijing Chemical Works. The 0.1 mol/L PBS buffered solution (pH 5.8) was used as the medium for detection process.

Apparatus

The fluorescence spectra were obtained by using a Shimadzu RF-5301 PC

View Article Online
DOI: 10.1039/C6AN01087C

spectrofluorophotometer equipped with a xenon lamp using right-angle geometry. UV-vis absorption spectra were obtained by a Varian GBC Cintra 10e UV-vis spectrometer. In both experiments, a 1 cm path-length quartz cuvette was used. FT-IR spectra were recorded with a Bruker IFS66V FT-IR spectrometer equipped with a DGTS detector. All pH measurements were made with a PHS-3C pH meter (Tuopu Co., Hangzhou, China). Transmission electron microscopy (TEM) experiments were performed on a Philips Tecnai F20 TEM operating at 200 KV acceleration voltage.

The preparation of GO by the modified Hummers method

Graphene oxide (GO) was prepared from graphite powder by the modified Hummers method.[13] Typically, 1.0 g of graphite powder was added to 25 mL H_2SO_4 (98%) and stirred 30 min. Afterwards, 3.5 g $KMnO_4$ was added and the mixture was stirred for 30min in an ice bath, and then stirred at 35 °C for 1h. Next, the mixture was diluted by 90 mL distilled water and the temperature was increased to 90 °C stirred for another 30 min. Subsequently, another 90 mL diluted water was added and then 10 mL of 30% H_2O_2 solution was added. The color of the mixture changed to bright yellow quickly. The resulting mixture was washed with distilled water several times and purified in a dialysis bag with a molecular weight cutoff of 10000 Da against deionized water until the pH of the solution became neutral. After that, the solution was dried under vacuum to remove water. Finally, some black GO powder was obtained.

The preparation of GQDs by the chemical oxidation of GO

1.0 g GO was dissolved in 30 mL H_2SO_4 (98%) and stirred 15 min, Afterwards, 5.0 g $KMnO_4$ was added and the mixture was stirred for 30min in an ice bath, and then stirred at 40 °C for 1h, Next, the mixture was diluted by slowly dropwise adding 120 mL distilled water, afterward, 10 mL of

View Article Online
DOI: 10.1039/C6AN01087C

30% H_2O_2 solution was added. The solution became transparent and color of the solution changed to bright yellow quickly. Finally, the solution was purified in a dialysis bag with a molecular weight cutoff of 1000 Da against deionized water to obtain a pure GQDs solution. Finally, the brightly orange GQDs solution was obtained. 500 μL GQDs was diluted to 2.0 mL with deionized water. The fluorescence spectra were recorded from 500 nm to 700 nm with the excitation wavelength of 470 nm. The slit widths of excitation and emission were both 10 nm.

The fluorescence quenching of GQDs by PDDA

A 0.75 mg mL^{-1} GQDs solution was prepared and stored under ambient condition. 0.1mol L^{-1} PBS buffer solution (pH 5.8, 150 μL), 500 μL GQDs and various amounts of PDDA were successively added into a 2 mL calibrated centrifuge tube. The mixtures were diluted to the 2.0 mL mark with deionized water and mixed thoroughly. Three minutes later, the fluorescence spectra were recorded from 500 nm to 700 nm with the excitation wavelength of 470 nm. The slit widths of excitation and emission were both 10 nm.

The fluorescence recovery of GQDs by $(NaPO_3)_6$

To study the effect of the $(NaPO_3)_6$ on the fluorescence of the GQDs/PDDA system, 500 μL GQDs solution and 22.5 μg mL^{-1} PDDA, 0.1 mol L^{-1} PBS buffer (pH 5.8, 150 μL) and different concentrations of $(NaPO_3)_6$ solution were sequentially added into the calibrated centrifuge tube and diluted to the 2.0 mL mark with deionized water, shaken thoroughly and equilibrated for 3 minutes. The fluorescence spectra were recorded from 490 nm to 700 nm with the excitation wavelength of 470 nm. The slit widths of excitation and emission were both 10 nm.

The detection of ACP

A typical ACP detection process was performed as follow. 0.1 mol L^{-1} PBS buffer (pH 5.8, 150

View Article Online
DOI: 10.1039/C6AN01087C

µL), 500 µL GQDs solution and 22.5 µg mL^{-1} PDDA were added to a 2 mL calibrated centrifuge tube, shaken thoroughly and equilibrated for 3 minutes. Afterword, 4.75 µmol mL^{-1} $(NaPO_3)_6$ and different concentrations of ACP were sequentially added to the calibrated centrifuge tube and diluted to the 2.0 mL mark with deionized water, shaken thoroughly and equilibrated for 40 minutes. All the above operational procedure was performed at 37 □. The fluorescence spectra were recorded from 500 nm to 700 nm with the excitation wavelength of 470 nm. The slit widths of excitation and emission were both 10 nm. The fluorescence intensity of the maximum emission peak was used for the quantitative analysis of the level of ACP. All data were collected from at least three independent measurements. The signal mean and standard deviation (expressed in terms of an error bar) could be determined and reported.

Detection of ACP in human blood serum

For serum samples detection, drug-free human blood samples were collected from healthy volunteer at the Hospital of Changchun China–Japan Union Hospital. All experiments were performed in compliance with the relevant laws and institutional guidelines. All the blood samples were obtained through venipuncture and centrifuged at 10000 rpm for 10 min after standing for 2 h at room temperature. The serum samples were diluted 10000-fold times with PBS solution before detection.

Results and discussion

Mechanism of the assay

View Article Online
DOI: 10.1039/C6AN01087C

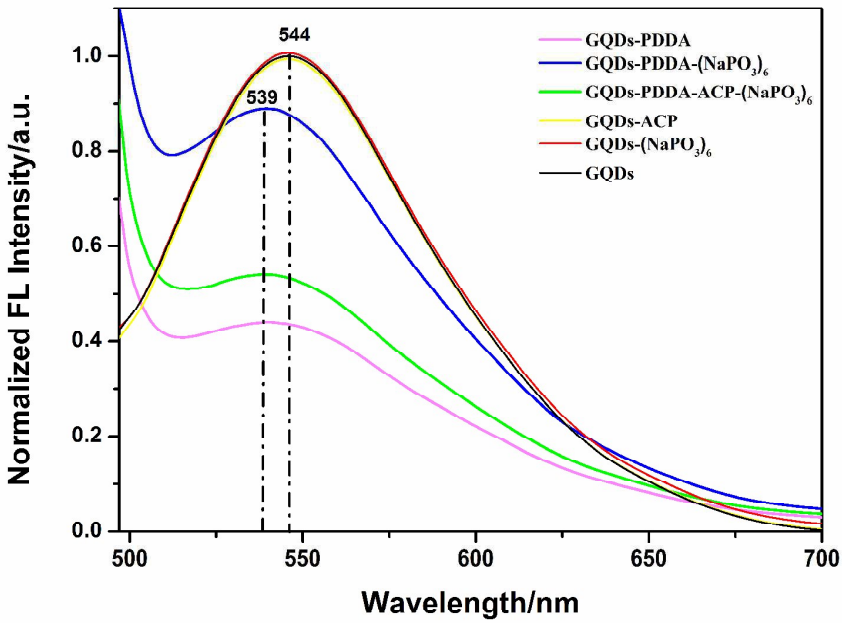

Fig. 1 The fluorescence spectra of GQDs, GQDs-$(NaPO_3)_6$, GQDs-ACP, GQDs-PDDA, GQDs-PDDA-$(NaPO_3)_6$ and GQDs-PDDA-ACP-$(NaPO_3)_6$ system. The concentations of $(NaPO_3)_6$, PDDA and ACP were 4.5 μmol mL^{-1}, 30 μg mL^{-1} and 500 nU mL^{-1}, respectively.

To get deeper insight into the detection mechanism of the GQDs-based biosensor, we studied the effect of $(NaPO_3)_6$, ACP, PDDA, PDDA-$(NaPO_3)_6$ and PDDA-ACP-$(NaPO_3)_6$ on the fluorescence of GQDs. As shown in Fig. 1 , there is no obviously change in fluorescence intensity of the GQDs after the addition of $(NaPO_3)_6$ or ACP, indicating both $(NaPO_3)_6$ and the ACP have no effect on the fluorescence of GQDs. The fluorescence of GQDs could be quenched by PDDA obviously and be recovered after the addition of $(NaPO_3)_6$, which attributed to the aggregation of PDDA/$(NaPO_3)_6$ complex and the disaggregation of the GQDs/PDDA complex by $(NaPO_3)_6$. From Fig. 1 we could also see a 5 nm blue shift was observed after the addition of PDDA to GQDs solution, which was a consequence of the change of quantum confinement of the GQDs and the modifications on the GQDs' surfaces caused by the binding of PDDA.[14-15] Furthermore, the fluorescence could be

View Article Online
DOI: 10.1039/C6AN01087C

quenched again after the addition of ACP to the GQDs/$(NaPO_3)_6$/PDDA system, indicating the $(NaPO_3)_6$ is hydrolyzed to the phosphate segments by ACP and the PDDA/$(NaPO_3)_6$ complex was distracted to form the GQDs/PDDA aggregates again.

Characterization of GQDs

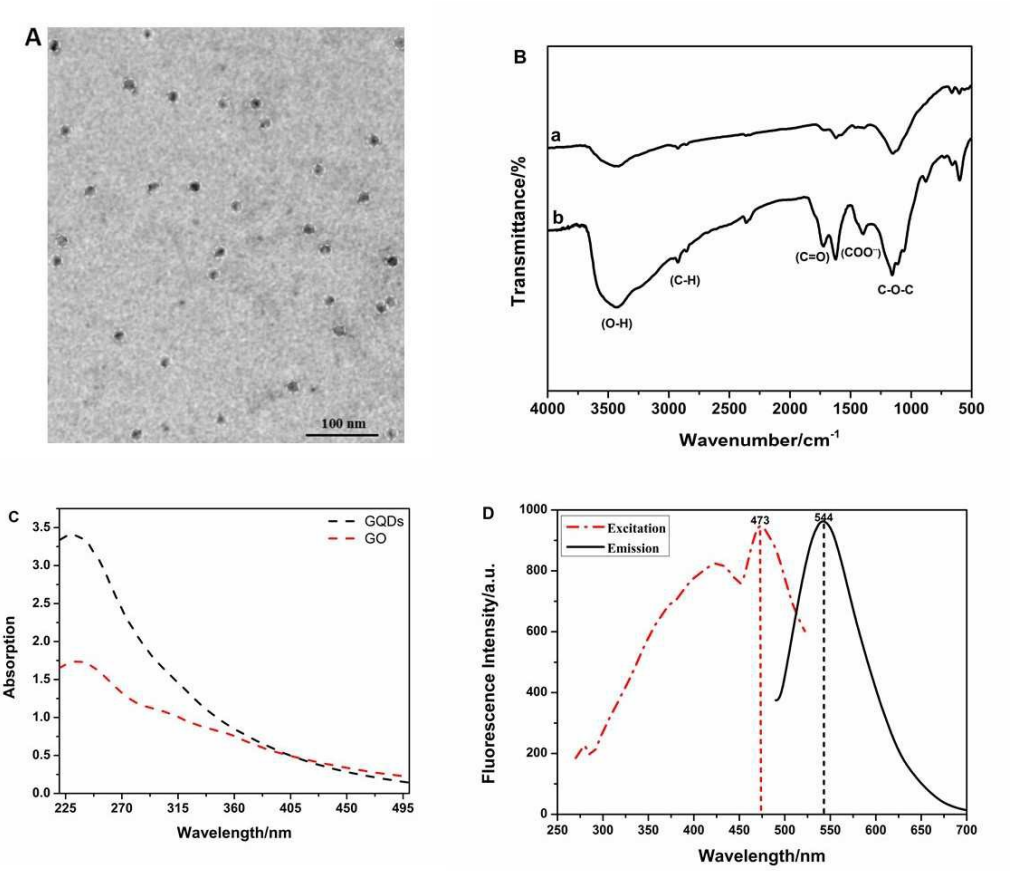

Fig. 2 (A) TEM images of GQDs. **(B)** The FT-IR spectra of GO (a) and GQDs (b). **(C)** UV/Vis absorption spectra of GO (red dash line) and GQDs (black dash line). **(D)** The excitation spectra (red dash line) and emission spectra (black solid line) of GQDs.

The transmission electron microscopy (TEM) image in Fig. 2(A) revealed the shape of GQDs was nearly spherical with the average diameter of 20 nm. The existence of surface functional groups of GQDs was studied by using FT-IR spectra (Fig. 2(B)). Peaks at 3200–3550 cm^{-1} and 2800–2950 cm^{-1} could be attributed to the C–OH and C–H stretching vibrations, respectively. Peaks at about

View Article Online
DOI: 10.1039/C6AN01087C

1600 cm^{-1} indicated the presence of C=O and the band at around 1080 cm^{-1} presents the existence of C–O (hydroxyl, ester, epoxide or ether) groups.[16-17] When compared with the relatively FI-TR intensity of GO, the oxidation degree of GQDs was much stronger which indicated GQDs contain more oxygen-containing groups on the surface. Generally, the existence of these functional groups represented excellent water solubility of these nanomaterials without further surface modification. As shown in Fig. 2(C), both GQDs and GO showed strong absorbance in the range of deep UV and a weak shoulder peak at about 300 nm, which was ascribed to π–π* transition of aromatic C=C bonds and n-π* transition of C=O bond, respectively.[18-19] The FI-TR and UV results indicated that the GQDs kept and had a GO nature. From Fig. 2(D), we could see the orange-fluorescent GQDs showed a symmetrical and broad fluorescence peak. The strongest fluorescence emission appeared at 544 nm upon 470 nm excitation.

The aggregation-caused quenching of GQDs by PDDA

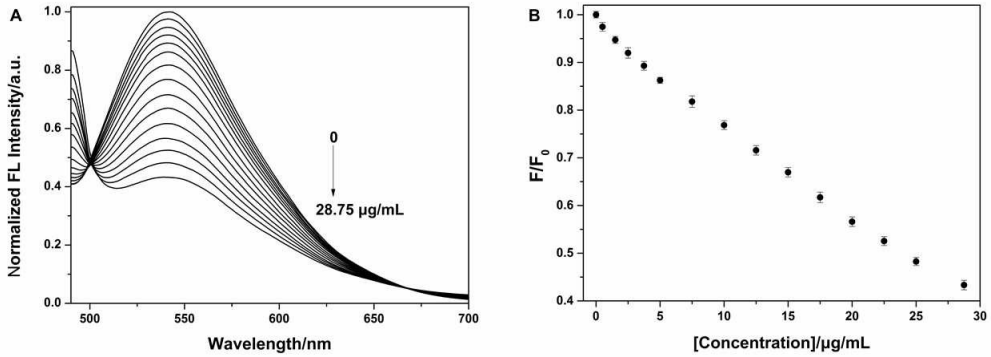

Fig. 3 (A) Fluorescence spectra of GQDs upon the addition of different concentrations of PDDA from 0 to 28.75 μg mL^{-1} (0, 0.5, 1.5, 2.5, 3.75, 5, 7.5, 10, 12.5, 15, 17.5, 20, 22.5, 25 and 28.75 μg mL^{-1}). **(B)** The plot of the relative fluorescence intensity versus the concentration of PDDA in the range of 0 to 28.75 μg mL^{-1}. PBS: 10 mmol L^{-1} (pH 5.8). (F_0 and F are the fluorescence intensity

View Article Online
DOI: 10.1039/C6AN01087C

of the GQDs in the absence and presence of PDDA, respectively).

PDDA with highly hydrophilic and permanently charged quaternary ammonium groups is a water-soluble cationic polyelectrolyte.[20] It contains many positively charged quaternary ammonium ions, which enables it to easily assemble with electronegative probes through electrostatic self-assembly.[21] In this work, we studied the response of GQDs to the different concentrations of PDDA. As shown in Fig. 3(A), upon stepwise addition of PDDA, the fluorescence intensity of GQDs was gradually decreased, which was due to the formation of GQDs/PDDA complex. Fig. 3(B) showed that there was a good linear relationship between the relative fluorescence intensity F/F_0 (F_0 and F are the fluorescence intensity of the GQDs in the absence and presence of PDDA, respectively) and the concentration of PDDA range from 0 to 28.75 μg mL^{-1}. Fig. S1 showed resonance light scattering (RLS) spectra of GQDs in the presence of different concentration of PDDA. It could be seen that the RLS intensity increased with the increase of the concentration of PDDA, indicating the diameter of GQDs in the presence of PDDA increased with the increase of PDDA concentration. The RLS enhancement was mainly due to the electrostatic interaction between the negatively charged GQDs and the positively charged PDDA, which could form GQDs/PDDA aggregates. So the fluorescence quenching was a result of the self-assembly of GQDs/PDDA. In this work, we chose 22.5 μg mL^{-1} PDDA to fabricate the biosensor for the further detection.

The fluorescence recovery induced by the $(NaPO_3)_6$

View Article Online
DOI: 10.1039/C6AN01087C

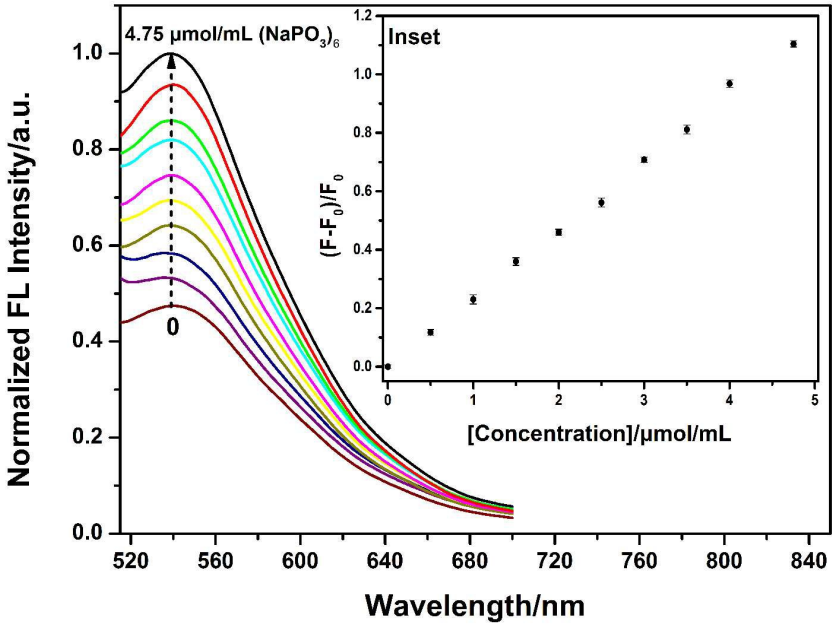

Fig. 4 Fluorescence spectra of GQDs upon the addition of different concentrations of $(NaPO_3)_6$ from 0 to 4.75 μmol mL^{-1} (0, 0.5, 1, 1.5, 2, 2.5, 3, 3.5, 4 and 4.75 μmol mL^{-1}) in the presence of 22.5 μg mL^{-1} PDDA. **Inset**: The relationship between $(F-F_0)/F_0$ and the concentration of $(NaPO_3)_6$ (from 0 to 4.75 μmol mL^{-1}). F_0 and F were the fluorescence intensity of GQDs/PDDA system in the absence and presence of $(NaPO_3)_6$. PDDA: 22.5 μg mL^{-1}, PBS: 10 mmol L^{-1} (pH 5.8).

An important feature of noncovalent self-assembly is the controllable aggregation/disaggregation of GQDs systems by chemical stimuli.[22] Such a process should be accompanied by the change in GQDs fluorescence, enabling the design of label-free biological sensors. $(NaPO_3)_6$ is highly negatively charged and is known to form strong complexes with the highly positively charged. We hypothesized that the stronger of this interaction should result in dissociation of the GQDs/PDDA complex upon addition of $(NaPO_3)_6$ and release of the GQDs. It can be seen from Fig. 4 that the PDDA-quenched fluorescence of GQDs could be gradually recovered with the increase of $(NaPO_3)_6$ concentration in the range from 0 to 4.75 μmol mL^{-1}. The inset of Fig. 4 showed that the

View Article Online
DOI: 10.1039/C6AN01087C

relationship between the recovery ratio $(F-F_0)/F_0$ of GQDs and $(NaPO_3)_6$ concentration in the range from 0 to 4.75 μmol mL^{-1}. As expected, $(NaPO_3)_6$ was found to restore the fluorescence of GQDs, which was due to its preferential binding with PDDA. The use of $(NaPO_3)_6$/PDDA complex to disrupt the GQDs/PDDA self-assembly was further exploited to the detection of ACP.

Optimization for ACP detection

In order to obtain a fluorescent biosensor with good sensing performance, we further optimized the experiment conditions. The effect of pH on the fluorescence intensity of GQDs system was initially studied. From Fig. S2, it can be seen that the fluorescence intensity of GQDs decreased when the pH of the medium was increased from acidic to basic conditions, The decrease in fluorescence intensity could be due to a decrease in the number of carboxyl-rich GQDs, which were being transformed into hydroxyl-rich GQDs as a result of the pH change.[23] Thus, the intermolecular H-bonding force could overcome the relatively low repulsive force in alkaline media, resulting in aggregation of GQDs. Moreover, most ACP require a lower pH for enzymatic activity. Under the weakly acidic condition, the ACP detection could not be disturbed by alkaline phosphatase.

As shown in Fig. S3, the effect of hydrolysis time on the ACP assay performance was investigated with three different ACP concentrations. We observed that the hydrolysis rate of $(NaPO_3)_6$ was increased with the enhancement of ACP concentration, and the fluorescence intensity of PDDA–GQDs–$(NaPO_3)_6$–ACP system obviously decreased with an increase in incubation time and tended to be constant after 40 min. To obtain an effective hydrolysis for an ACP assay, pH 5.8 and 40 min of hydrolysis time was used in the further ACP assay. We also investigated the effect of incubation temperature on the hydrolysis of $(NaPO_3)_6$ by ACP. The result in Fig. S4 showed that

View Article Online
DOI: 10.1039/C6AN01087C

the relative fluorescence intensity (F/F_0) of GQDs-PDDA-$(NaPO_3)_6$-ACP system (F_0 and F are the fluorescence intensities of the PDDA–GQDs–$(NaPO_3)_6$ system in absence and presence of ACP) at 37 □ was the lowest, which was consistent with the optimum temperature of the catalytic behavior of ACP. So we chose 37 □ as the optimal incubation temperature in the further experiments.

The detection of ACP

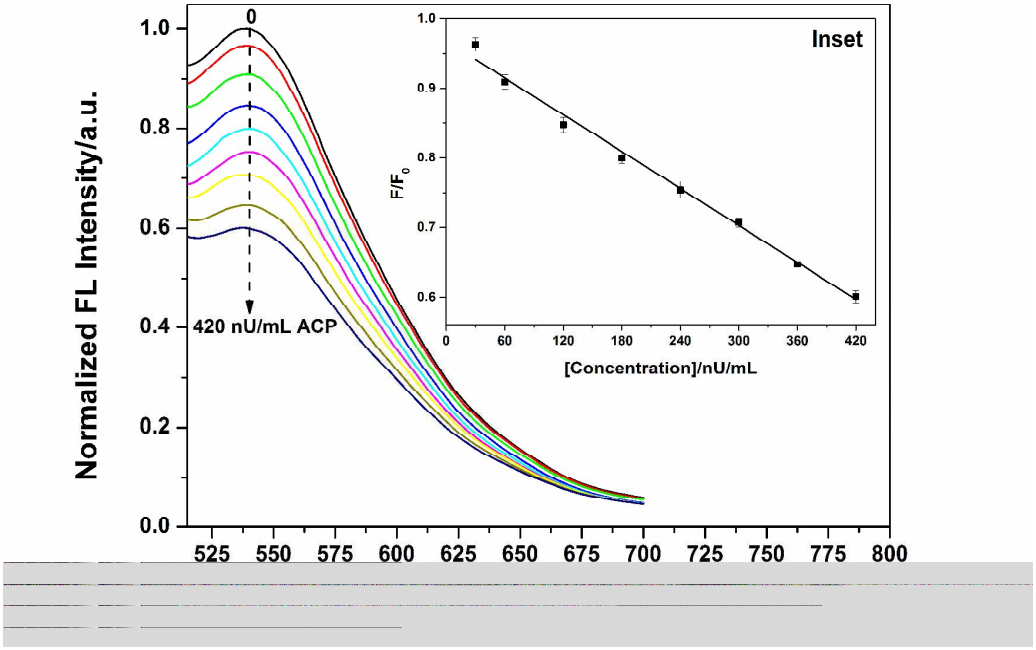

Fig. 5 The fluorescence spectra of GQDs-PDDA-$(NaPO_3)_6$ sensing system in the presence of different concentrations of ACP (0, 30, 60, 120, 180, 240, 300, 360 and 420 nU mL^{-1}). **Inset** shows the linear relationship between F/F_0 and the concentration of ACP (from 30 to 420 nU mL^{-1}). F_0 and F is the fluorescence intensity of GQDs-PDDA-$(NaPO_3)_6$ system before and after the addition of ACP, respectively. Reaction conditions: 10 mmol/L PBS buffer solution (pH 5.8), incubated for 40 min.

In the presence of ACP, $(NaPO_3)_6$ was hydrolyzed to inorganic phosphate ions, whose weak

View Article Online
DOI: 10.1039/C6AN01087C

interaction with PDDA could cause the dissociation of the $(NaPO_3)_6$/PDDA aggregates. Fig. 5 was the fluorescence spectra of GQDs-PDDA-$(NaPO_3)_6$ system in the presence of different concentrations of ACP. We can observe that the fluorescence intensity of sensing system in the absence of ACP was quite strong. After the introduction of ACP to the sensing system, the fluorescence intensity gradually decreased with increasing the concentration of ACP, indicating the transformation of GQDs from monemer to GQDs/PDDA aggregates again. Fig. 5 Inset showed that there was a good linear relationship between F/F_0 and ACP concentration in the range from 30 nU mL^{-1} to 420 nU mL^{-1}. The regression equation is $F/F_0 = 0.96772 - 0.00088$ [ACP], nU mL^{-1}. The corresponding regression coefficient (R^2) is 0.9911, and the detection limit for ACP is 12 nU mL^{-1}. Some analytical parameters in other methods for the detection of ACP were listed in Table S1.[1, 5, 8, 24-25] Compared with those reports about ACP assay, our present method offered a comparable or super detection limit and linear range.

Interference Study

Under optimized experimental conditions, the selectivity of the developed method was evaluated by using ACP (420 nU mL^{-1}) and other 9 common proteins, including ALP, lysozyme, BHB, BSA, HRP, trypsin, pepsin and thrombin (Fig. S5). The results showed that only ACP could cause the significant fluorescence quenching of GQDs-PDDA-$(NaPO_3)_6$ system, while the presence of other proteins have a neglect influence on the fluorescence intensity compared to the blank test (in the absence of proteins). Moreover, we further evaluated the selectivity of our method with various coexisting ions added. Table S2 showed the interference effect of some common inorganic ions on the determination of ACP (300 nU mL^{-1}), a relative error of 5.0% was considered to be tolerable. As shown in Table S2, the tolerable concentration of NaCl, KCl, $MgCl_2$, $Zn(NO_3)_2$, $Ca(NO_3)_2$,

View Article Online
DOI: 10.1039/C6AN01087C

Na_3PO_4, Na_2HPO_4 and NaH_2PO_4 was 10.00 μmol mL^{-1}. The concentration of $FeCl_3$ and $FeCl_2$ was 0.1 and 2 μmol mL^{-1}, respectively. These results shows the high selectivity of the method. Therefore, this biosensor had the specific ability of sensing ACP in the presence of other common proteins.

Detection of ACP in human serum samples

Table 1 Results of ACP determination in human serum samples

Sample	Original found (μU mL^{-1})	Added (μU mL^{-1})	Total found (μU mL^{-1})	Recovery (%)	RSD (n=3, %)
0	0.262	0.00	0.262±0.009	——	3.4
1	0.264	0.08	0.337±0.005	97.97	3.9
2	0.271	0.10	0.365±0.002	98.38	2.7
3	0.253	0.12	0.369±0.004	98.92	3.1

To assess the application of this biosensor in complex biological systems, the analysis of ACP in human serum samples were carried out. Serum is what remains from whole blood after coagulation, the chemical composition is similar to plasma but does not contain coagulation protein. We performed detection of ACP in serum samples under the optimal conditions. The results obtained by standard addition method were listed in Table 1. From Table 1, we can see that the RSD was lower than 3.9% and the average recoveries of ACP in the real samples were in the range of 97.97–98.92%, which indicating that the accuracy and precision of the proposed method were satisfactory.

Conclusion

A simple, facile and top-down chemical synthetic route was developed to prepare GQDs with orange fluorescence emission. GQDs with aggregation-caused quenching characteristics are

View Article Online
DOI: 10.1039/C6AN01087C

weakly fluorescent in their aggregate states. The integration of GQDs and PDDA via self-assembly offers a flexible tool kit for the design of label-free biosensor for ACP. On the one hand, $(NaPO_3)_6$ with strong negative charge could competitively bind to PDDA and disassociate GQDs/PDDA aggregates. On the other hand, $(NaPO_3)_6$ could be hydrolyzed into phosphate segments by ACP under acidic environment. Thus, ACP sensing and discrimination was achieved via the controlled self-assembly of GQDs. This sensing system could also be generalized to detect other ACPs, such as prostatic acid phosphatase, for further application in disease diagnosis and evaluation.

Acknowledgments

This work was financially supported by the National Natural Science Foundation of China (Nos. 21075050 and 21275063), the Science and Technology Development project of Jilin province, China (No. 20150204010GX)

References

1 J. Sun, F. Yang and X. Yang, *Nanoscale*, 2015, **7**, 16372-16380.

2 Z. Qian, L. Chai, Q. Zhou, Y. Huang, C. Tang, J. Chen and H. Feng, *Analytical chemistry*, 2015, **87**, 7332-7339.

3 Z. Lin, Z. Liu, H. Zhang and X. Su, *Analyst*, 2015, **140**, 1629-163

4 E. Koller and O. S. Wolfbeis, *Analytical biochemistry*, 1984, **143**, 146-151.

5 P. Guo, S. Yan, Y. Zhou, C. Wang, X. Xu, X. Weng and X. Zhou, *Analyst*, 2013, **138**, 3365-3367.

6 A. H. Kamel, H. R. Galal and A. A. Hanna, *International Journal of Electrochemical Science*, 2014, **9**, 5776-5787.

View Article Online
DOI: 10.1039/C6AN01087C

7 P. Calvo-Marzal, S. S. Rosatto, P. A. Granjeiro, H. Aoyama and L. T. Kubota, *Analytica Chimica Acta*, 2001, **441**, 207-214.

8 Z. Liu, Z. Lin, L. Liu and X. Su, *Analytica Chimica Acta*, 2015, **876**, 83-90.

9 Y. Xu, B. Li, L. Xiao, J. Ouyang, S. Sun and Y. Pang, *Chemical Communications*, 2014, **50**, 8677-8680.

10 X. Yan, T. Hu, L. Wang, L. Zhang and X. Su, *Biosensors & Bioelectronics*, 2016, **79**, 922-929.

11 S. Zhu, N. Zhou, Z. Hao, S. Maharjan, X. Zhao, Y. Song, B. Sun, K. Zhang, J. Zhang, H. Sun, L. Lu and B. Yang, *Rsc Advances*, 2015, **5**, 39399-39403.

12 H. Zhou, F. Zou, T. Van Tan and J. Lee, *Rsc Advances*, 2015, **5**, 81753-81758.

13 W. S. Hummers and R. E. Offeman, *Journal of the American Chemical Society*, 1958, **80**, 1339-1339.

14 P. E. Cabral Filho, M. I. A. Pereira, H. P. Fernandes, A. A. de Thomaz, C. L. Cesar, B. S. Santos, M. L. Barjas-Castro and A. Fontes, *International Journal of Nanomedicine*, 2015, **10**, 4393-4404.

15 B. B. Campos, M. Algarra, B. Alonso, C. M. Casado,J. C. G. Esteves da Silva, *Analyst*, 2009, **12**, 2447-2452.

16 N. Yu, H. Peng, H. Xiong, X. Wu, X. Wang, Y. Li and L. Chen, *Microchimica Acta*, 2015, **182**, 2139-2146.

17 S. Weng, D. Liang, H. Qiu, Z. Liu, Z. Lin, Z. Zheng, A. Liu, W. Chen and X. Lin, *Sensors and Actuators B-Chemical,* 2015, **221**, 7-14.

18 X. Tan, Y. Li, X. Li, S. Zhou, L. Fan and S. Yang, *Chemical Communications*, 2015, **51**, 2544-2546.

19 Y. Liu and D. Y. Kim, *Chemical communications (Cambridge, England)*, 2015, **51**, 4176-4179.

20 J. Chen, Y. Lin, Y. Wang and L. Jia, *Journal of Chromatography B-Analytical Technologies in the Biomedical and Life Sciences*, 2015, **991**, 59-67.

21 R. Yang, X. Ding, Y. Zhou, J. Li, L. Qu and K. Zhang, *Analytical Methods*, 2015, **7**, 436-442.

22 Y. Lin, R. Chapman and M. M. Stevens, *Advanced Functional Materials*, 2015, **25**, 3183-3192.

View Article Online
DOI: 10.1039/C6AN01087C

23 T. Ghosh and E. Prasad, *Journal of Physical Chemistry C*, 2015, **119**, 2733-2742.

24 A. K. Dwivedi and P. K. Iyer, *Analytical Methods*, 2013, **5**, 2374-2378.

25 Y. Xie, Y. Tan, R. Liu, R. Zhao, C. Tan and Y. Jiang, *ACS Appl Mater Interfaces*, 2012, **4**, 3784-3787.

View Article Online
DOI: 10.1039/C6AN01087C

Graphic Abstract

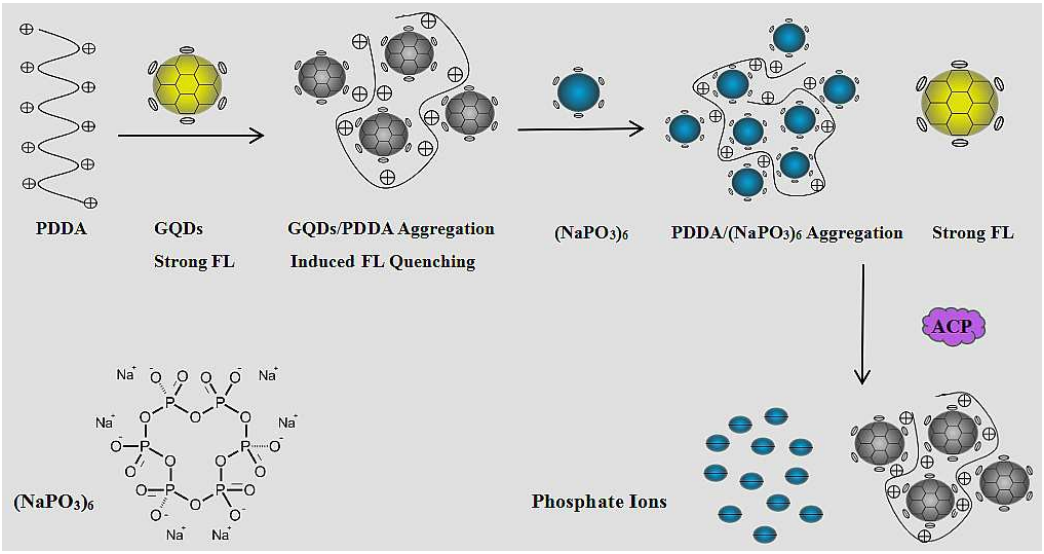

The presentation of the mechanism for the detection of ACP based on the aggregation of GQDs